


Optimal Resetting Brownian Bridges via Enhanced Fluctuations

Benjamin De Bruyne¹, Satya N. Majumdar¹ and Grégory Schehr²

¹LPTMS, CNRS, Univ. Paris-Sud, Université Paris-Saclay, 91405 Orsay, France

²Sorbonne Université, Laboratoire de Physique Théorique et Hautes Energies, CNRS UMR 7589, 4 Place Jussieu, 75252 Paris Cedex 05, France

 (Received 6 January 2022; revised 6 April 2022; accepted 25 April 2022; published 17 May 2022)

We introduce a resetting Brownian bridge as a simple model to study search processes where the total search time t_f is finite and the searcher returns to its starting point at t_f . This is simply a Brownian motion with a Poissonian resetting rate r to the origin which is constrained to start and end at the origin at time t_f . We unveil a surprising general mechanism that enhances fluctuations of a Brownian bridge, by introducing a small amount of resetting. This is verified for different observables, such as the mean-square displacement, the hitting probability of a fixed target and the expected maximum. This mechanism, valid for a Brownian bridge in arbitrary dimensions, leads to a finite optimal resetting rate that minimizes the time to search a fixed target. The physical reason behind an optimal resetting rate in this case is entirely different from that of resetting Brownian motions without the bridge constraint. We also derive an exact effective Langevin equation that generates numerically the trajectories of a resetting Brownian bridge in all dimensions via a completely rejection-free algorithm.

DOI: 10.1103/PhysRevLett.128.200603

Search processes are ubiquitous in nature. They appear in a wide range of situations ranging from foraging animals [1,2], biochemical reactions [3–6], and all the way to behavioral psychology [7–9]. Search problems exhibit rich features [10–15] and finding an optimal search strategy in a given context is an interesting problem with multiple applications across disciplines [16,17]. In recent years, there has been a surge of interest in the effect of resetting in search processes (for a recent review see Ref. [18]). Stopping and starting from scratch has shown to be an efficient search strategy in several contexts such as in optimization algorithms [19–23], chemical reactions [24,25], animal foraging [26–30], and catastrophes in population dynamics [31–40]. Perhaps the effect of resetting is best seen in the simple model of diffusion introduced by Evans and Majumdar [41,42]. In this resetting Brownian motion (RBM) model, the position $x(t)$ of a Brownian motion, e.g., in one dimension, is reset to the origin randomly in time according to a Poisson process with a constant rate r . In a time interval dt , the position $x(t)$ follows the stochastic rule

$$x(t + dt) = \begin{cases} x(t) + \sqrt{2D}\eta(t)dt, & \text{with prob. } 1 - rdt, \\ 0, & \text{with prob. } rdt, \end{cases} \quad (1)$$

where D is the diffusion coefficient and $\eta(t)$ is an uncorrelated white noise with zero mean $\langle \eta(t) \rangle = 0$ and delta correlator $\langle \eta(t)\eta(t') \rangle = \delta(t - t')$. The dynamics therefore consists of a combination of pure diffusion with

intermittent resets to the origin. The effect of resetting on the search process can be simply measured by the mean first-passage time $\langle T(M) \rangle$ to a level M , which is the mean time the searcher takes to find a target located at a position M . For pure diffusion without resetting, it is well known that this quantity is infinite [43,44]. In contrast, resetting leads to the striking result that the mean first-passage time $\langle T(M) \rangle$ becomes not only finite but also that it becomes minimal at an optimal resetting rate r^* . The mechanism behind this result is that resetting suppresses the trajectories that diffuse far away from the target and makes them restart from the origin, hence increasing their chances to find the target. This model is straightforward to generalize to higher dimensions and an optimal resetting rate has been shown to exist in all dimensions [45]. Since the original model, the existence of an optimal resetting rate has been studied extensively for various stochastic processes, leading to a tremendous amount of activities [42,45–63]—see Ref. [18] for a review. The existence of this optimal resetting rate has also been confirmed in experiments with optical traps in both one and two dimensions [64–66].

In most studied examples of search processes with resetting, the underlying search process is assumed to be *free*, i.e., it does not satisfy additional constraints. However, in many circumstances, search processes are typically time-limited and do not have the luxury to continue forever. For example, while foraging for food, animals typically start from their nest and come back to it at the end of the day [26,28,30,67–76]. Search patterns may vary from species to species. For example, desert ants such as *Cataglyphis fortis* explore space in a rather tortuous manner, but return home

(inbound) almost along a straight line [73]. Another typical example of a time-limited search occurs in a rescue mission after a plane crash in the ocean: the divers are typically called off after a certain amount of time and they go back to their initial location. The stochastic moves in such search processes may be situation specific, but they all share a common feature; namely, they are constrained to come back to their starting point after a fixed time t_f , the so called *bridge* condition. Our goal in this Letter is not to provide an accurate description of a specific search process, but rather to study the combined effect of *resetting* and the *bridge constraint* in a simple solvable search process to gain interesting insights. An ideal setting for such a simple solvable model is provided by a *Brownian bridge*, where the process undergoes a Brownian motion locally in time, but is constrained to reach a fixed position (e.g., the initial position) after a fixed time t_f . Brownian bridges have been studied extensively with many applications. For example, they play an important role in analyzing animal movements: typically the positions of an animal are recorded by GPS at discrete times and the trajectory in between two successive recorded positions is approximated by a Brownian bridge within the popular Brownian bridge movement model (BBMM) [74]. This, in turn, has been used to characterize the home ranges of birds [75]. A similar construction is used in a completely different context of finance, e.g., in the valuation of a mortgage-backed security portfolio or the barrier options with a fixed maturity period t_f [76]. Brownian bridges also appear as central objects in statistical inference, e.g., in the celebrated Kolmogorov-Smirnov distribution-free test for the independence of random variables [77].

In this Letter, we study a Brownian bridge model in arbitrary dimensions with a fixed duration t_f , but in the presence of *resetting* at a constant rate r to its initial position. We call this a *resetting* Brownian bridge (RBB), with $\mathbf{x}_B(t)$ denoting its coordinate at time $0 \leq t \leq t_f$ with the bridge conditions $\mathbf{x}_B(0) = 0$ and $\mathbf{x}_B(t_f) = \mathbf{x}_f$. The general question we address is, is resetting still a good search strategy in the presence of a bridge constraint? In other words, does the paradigm of an optimal resetting rate r^* still hold for RBB? We find, rather surprisingly, that there is an interesting trade-off between resetting and the bridge constraint such that a small resetting rate, in the presence of a bridge constraint, actually *enhances* bridge fluctuations, rather than *reducing* it as naive expectations would suggest.

This “enhanced fluctuations mechanism” (EFM) of a Brownian bridge induced by resetting turns out to be rather general and holds in all dimensions. The origin of EFM can be qualitatively understood as follows. In the absence of resetting, the particle cannot go too far away from the origin, since it has to come back to the final position close to the origin at time t_f , by a slow diffusing process. However, when a small amount of resetting rate r is

switched on, the particle can go further away from the origin since it can come back close to the origin at time $t = t_f$ by a “last minute” instantaneous resetting. Hence there is a subtle trade-off between the resetting and the bridge constraint. Clearly, this argument is rather general and is expected to hold in any dimension, as demonstrated in Sec. III of the Supplemental Material [78]. For the purpose of clarity, we will present mostly the $1d$ case in the main text, and defer the details for $d > 1$ to Ref. [78].

The EFM has important consequences for search processes. If a target is placed at a fixed distance from the origin where the searcher starts, resets, and returns, a bigger spatial fluctuation of the searcher would imply that the target will be found more easily. Indeed, we also compute exactly the probability to find the target before t_f (hitting probability) and show that it also has a nonmonotonic behavior as a function of r , achieving its maximum at an optimal resetting rate. Computations of other observables, such as the expected maximum of the RBB, also confirms the existence of an optimal resetting rate. Thus the paradigm of the existence of an optimal resetting rate also holds for constrained bridge processes with resetting, albeit the physical mechanism at play is rather different from the free case. In addition to unveiling this general *fluctuations enhancing* mechanism via resetting and a bridge constraint, we also address an important algorithmic issue: how does one generate a Brownian bridge with resetting numerically in an efficient manner? In this Letter, we show how to derive an effective Langevin equation that allows us to generate RBB trajectories with the correct statistical weight in a completely *rejection-free* manner.

Our first goal is to construct a rejection-free algorithm to generate an RBB with the correct statistical weight. Even though this algorithm can be derived in all dimensions d [78], here we present the $d = 1$ case where, for simplicity, we set the initial and final positions of the bridge to be the same, namely, $x_B(t_f) = x_B(0) = 0$. Generating constrained stochastic Markov processes was initially studied in the probability literature [82,83] and more recently it has emerged as a vibrant research area by itself in the context of sampling rare or constrained trajectories with applications ranging from chemistry and biology all the way to particle physics [84–103]. In the context of the RBB, a naive solution would be to generate free RBM paths and discard the ones that do not satisfy the bridge constraint $x_B(t_f) = 0$. However, this is computationally wasteful since the RBM trajectories that go back to the vicinity of 0 at $t = t_f$ are typically rare. Here, we show that the RBB trajectories can be generated in a rejection-free manner, from the effective Langevin equation

$$x_B(t + dt) = \begin{cases} x_B(t) + \sqrt{2D}\eta dt + \tilde{\mu}dt, & p = 1 - \tilde{r}dt, \\ 0, & p = \tilde{r}dt, \end{cases} \quad (2)$$

where the effective drift $\tilde{\mu}$ and resetting rate \tilde{r} are space-time dependent and are given by

$$\tilde{\mu}(x_B, t) = -\sqrt{4rD}\mathcal{V}(y, \tau), \quad (3a)$$

$$\tilde{r}(x_B, t) = r\mathcal{W}(y, \tau), \quad (3b)$$

with $y = x_B/\sqrt{4D(t_f - t)}$, $\tau = r(t_f - t)$ and the scaling functions

$$\mathcal{V}(y, \tau) = \frac{ye^{-y^2-\tau}}{\sqrt{\tau}[e^{-\tau-y^2} + \sqrt{\pi\tau}\text{erf}(\sqrt{\tau})]}, \quad (4a)$$

$$\mathcal{W}(y, \tau) = \frac{e^{-\tau} + \sqrt{\pi\tau}\text{erf}(\sqrt{\tau})}{e^{-\tau-y^2} + \sqrt{\pi\tau}\text{erf}(\sqrt{\tau})}. \quad (4b)$$

Here $\text{erf}(z) = (2/\sqrt{\pi}) \int_0^z e^{-u^2} du$ is the error function. Note that while RBM with space-time dependent resetting rates have been studied before [18,42,104–108], here they emerge naturally and have a specific form in order to satisfy the bridge constraint.

To derive this effective Langevin equation (2), we consider the probability distribution function (PDF) $P_B(x, t|t_f)$ of the position $x_B(t)$ of an RBB of total duration t_f . We split the interval $[0, t_f]$ into two parts: $[0, t]$ and $[t, t_f]$ and use the Markov property of the bridge to write

$$P_B(x, t|t_f) = \frac{P_r(x, t|0, 0)P_r(0, t_f|x, t)}{P_r(0, t_f|0, 0)}, \quad (5)$$

where $P_r(x, t|0, 0)$ is the PDF of the RBM at time t , starting from the origin at $t = 0$. The denominator is just a normalization constant that ‘‘counts’’ all the trajectories of the RBM of duration t_f , starting and ending at 0. Note that Eq. (5) can be interpreted as the fraction of all RBM paths of duration t_f satisfying the bridge constraint that also pass through x at time t . To ease notation, we introduce the *forward* propagator $P_r(x, t) \equiv P_r(x, t|0, 0)$, where x appears as the final position, and the *backward* propagator $Q_r(x, t) \equiv P_r(0, t_f|x, t)$, where x appears as the initial position. In these notations, Eq. (5) reads $P_B(x, t|t_f) = P_r(x, t)Q_r(x, t)/P_r(0, t_f)$. The two quantities $P_r(x, t)$ and $Q_r(x, t)$ satisfy, respectively, the forward and backward Fokker-Plank equations of RBM, respectively, given by (see Supplemental Material [78] for details)

$$\partial_t P_r(x, t) = D\partial_{xx}P_r(x, t) - rP_r(x, t) + r\delta(x), \quad (6a)$$

$$-\partial_t Q_r(x, t) = D\partial_{xx}Q_r(x, t) - rQ_r(x, t) + rQ_r(0, t), \quad (6b)$$

with the initial and final conditions $P_r(x, 0) = \delta(x)$, $Q_r(x, t_f) = \delta(x)$. Our goal is to write the Fokker-Plank equation satisfied by the bridge PDF $P_B(x, t|t_f)$. Taking a

time derivative of Eq. (5) and using Eqs. (6) satisfied by the free propagators, we get [see Eq. (21) of Ref. [78] with $d = 1$]

$$\begin{aligned} \partial_t P_B(x, t|t_f) &= D\partial_{xx}P_B(x, t|t_f) - \partial_x[\tilde{\mu}(x, t)P_B(x, t|t_f)] \\ &\quad - \tilde{r}(x, t)P_B(x, t|t_f) + \delta(x) \int_{-\infty}^{\infty} \tilde{r}(x', t)P_B(x', t)dx', \end{aligned} \quad (7)$$

where we have introduced an effective space-time dependent drift $\tilde{\mu}(x, t)$ and resetting rate $\tilde{r}(x, t)$ which are given by

$$\tilde{\mu}(x, t) = 2D\partial_x \ln[Q_r(x, t)]; \quad \tilde{r}(x, t) = r \frac{Q_r(0, t)}{Q_r(x, t)}. \quad (8)$$

From the Fokker-Planck equation (7), one can derive the effective Langevin equation (2), as explained in Sec. II of Ref. [78]. To compute $\tilde{\mu}(x, t)$ and $\tilde{r}(x, t)$, we need to compute the backward propagator $Q_r(x, t)$ in Eq. (8). Noting that $Q_r(x, t) = P_r(0, t_f|x, t)$, we just need the propagator for the RBM, which can be computed by using the renewal identity [18]

$$\begin{aligned} P_r(x, t|x_0, 0) &= e^{-rt}P_0(x, t|x_0, 0) \\ &\quad + r \int_0^t d\tau e^{-r\tau}P_0(x, \tau|0, 0), \end{aligned} \quad (9)$$

where $P_0(x, t|x_0, 0) = e^{-[(x-x_0)^2/4Dt]}/\sqrt{4\pi Dt}$ is the standard Brownian propagator (without resetting). The renewal identity (9) simply states that for the particle to be at x at a time t , it either (i) must never reset, in which case its probability distribution is just the one of a free Brownian motion $P_0(x, t|x_0, 0)$, or (ii), reset for the last time at $t - \tau > 0$, after which the particle restarts from the origin and then propagates to x in the remaining time τ . As the resetting times follow a Poisson process, the former event happens with probability e^{-rt} while the latter happens with probability $re^{-r\tau}$ and has to be summed over all τ in $[0, t]$. From the renewal identity, one can straightforwardly obtain $Q_r(x, t) \equiv P_r(0, t_f|x, t)$ and then, using Eq. (8), find the exact expressions for $\tilde{\mu}(x, t)$ and $\tilde{r}(x, t)$ as given in Eqs. (3) and (4). We can then use Eq. (2) to generate RBB trajectories (see left panel in Fig. 1). The position distribution $P_B(x, t|t_f)$ obtained numerically is in excellent agreement with the theoretical one (see the right panel in Fig. 1). The effective Langevin equation (2) derived for the one-dimensional RBB can be generalized to RBB in higher dimensions in a rather straightforward manner, as detailed in Ref. [78]. Below we compute three observables illustrating the EFM exhibited by the RBB as a search process.

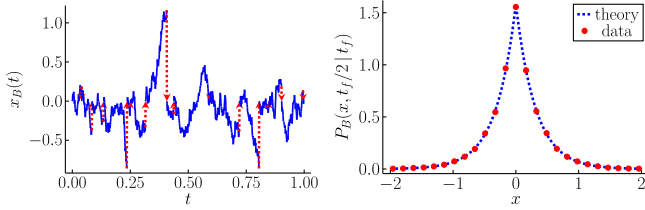


FIG. 1. Left: A typical RBB trajectory $x_B(t)$ with resetting rate $r = 10$, diffusion constant $D = 1$, and duration $t_f = 1$. The resetting events are denoted by red dashed lines with arrows. Right: Position distribution for an RBB at an intermediate time $t = t_f/2$, where $r = 10$, $D = 1$, and $t_f = 1$. The distribution obtained numerically by sampling the trajectories from the effective Langevin equation in Eq. (2) is compared with the theoretical prediction in Eq. (5)—see Eq. (35) in Ref. [78] for a more explicit expression. The histogram has been obtained by sampling 10^5 trajectories with uniform bin sizes of width 8×10^{-2} (only one of every two points are shown for clarity).

Mean square displacement.—The PDF of the position $x_B(t)$ of an RBB at some intermediate time $0 \leq t \leq t_f$ is given in Eq. (5). The mean position $\langle x_B \rangle(t|t_f)$ vanishes by symmetry. Hence the minimal quantity that characterizes the spatial fluctuations is the second moment of the PDF, i.e., the mean-square displacement $\langle x_B^2 \rangle(t|t_f)$. We compute $\langle x_B^2 \rangle(t|t_f)$ from Eq. (5) analytically, leading to

$$\langle x_B^2 \rangle(t|t_f) = 2Dt_f f\left(a = \frac{t}{t_f} R = rt_f\right), \quad (10)$$

where the scaling function f can be obtained explicitly [see Eq. (39) in Ref. [78]]. A plot of the function $f(a|R)$ vs $a \in [0, 1]$, for different values of R , is given in the left panel in Fig. 2. As the rescaled resetting rate $R = rt_f$ varies from 0 to ∞ , the function $f(a|R)$, crosses over from a parabolic to a flat shape, i.e., $f(a|R \rightarrow 0) = a(1-a)$ and $f(a|R \rightarrow \infty) \approx 1/R$. For a general R , the function

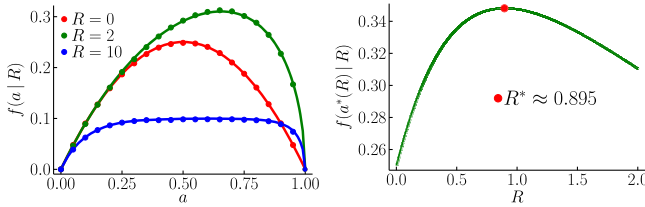


FIG. 2. Left panel: The function $f(a|R)$ plotted vs a is evaluated numerically, averaging over 10^5 samples, using the effective Langevin equation in Eq. (2) (symbols) and is compared to the theoretical prediction (plain lines), given in Eq. (10), for different values of R —see also Eqs. (39) and (41) in Ref. [78]. This function is clearly asymmetric around $a = 1/2$. Only when $R \rightarrow 0$, it approaches to the symmetric form $f(a|R \rightarrow 0) = a(1-a)$. For any R , the function $f(a|R)$ has a unique maximum at $a = a^*(R)$. Right panel: The maximal value $f(a^*(R)|R)$ plotted vs R . It has a unique maximum at $R^* \approx 0.895$ (red dot).

$f(a|R)$ is not symmetric around $a = 1/2$, since resetting breaks the time-reversal symmetry. For a given R , the function $f(a|R)$ has a unique maximum at $a = a^*(R)$ and this maximal mean square displacement $f(a^*(R)|R)$ (in units of $2Dt_f$) varies nonmonotonically with R : it first increases with increasing R , achieves a maximum at $R = R^* \approx 0.895$ and then decreases again with increasing R (see Fig. 2). Thus, interestingly, a nonzero resetting rate, when it is not too large, actually enhances the bridge fluctuations. Naively, one would think that resetting to the origin localizes the trajectory of the bridge in the vicinity of $x = 0$ and thus would suppress fluctuations. This naive picture holds only for very large R . Moreover, there is a nontrivial optimal rescaled resetting rate R^* that optimizes the maximum value of the mean-square displacement $f[a^*(R)|R]$ over the full interval $[0, t_f]$, thus enabling the particle to explore more space. Thus the EFM leading to an optimal r^* in the RBB is thus very different from the one in the free RBM.

Hitting probability.—To illustrate further the EFM in the context of a search of a target located at M , we next compute the hitting probability, i.e., the probability that the RBB (searcher) finds the target at M before time t_f . The hitting probability can be computed from the relation

$$p_{\text{hit}}(t_f, M) = \int_0^{t_f} dt F_B(t|M, t_f), \quad (11)$$

where $F_B(t|M, t_f)$ is the first-passage probability density of the RBB at level M with $t \leq t_f$. This can be computed by decomposing the RBB trajectories into two parts: one in the time interval $[0, t]$ where it first hits the level M at a time $t < t_f$, another one in the time interval $[t, t_f]$ where it propagates from M to the origin. One gets

$$F_B(t|M, t_f) = \frac{F_r(t|M)P_r(0, t_f|M, t)}{P_r(0, t_f|0, 0)}, \quad (12)$$

where $F_r(t|M)$ is the first-passage time distribution of a RBM [41], $P_r(x, t|x_0, t)$ is the propagator of a RBM given in Eq. (9) and the denominator is a normalization factor that “counts” all the bridge trajectories. Using the known results for $F_r(t|M)$ [41] and the propagator from Eq. (9) (see Ref. [78] for details) we get

$$p_{\text{hit}}(t_f, M) = h\left(R = rt_f, m = \frac{M}{\sqrt{2Dt_f}}\right), \quad (13)$$

where the scaling function h can also be computed analytically (see Sec. IV B in Ref. [78]). When $R = 0$, we recover the hitting probability of a Brownian bridge $h(R = 0, m) = e^{-2m^2}$. For a given target position m , the function $h(R, m)$ varies nonmonotonically with R and achieves a maximum at $R = R^*(m)$. A plot of $h(R, m)$ vs R for $m = 1$ is shown in the left panel in Fig. 3. Thus the

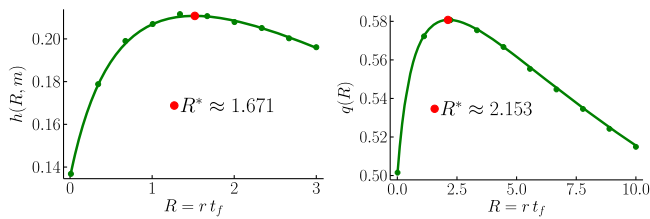


FIG. 3. Left panel: The theoretical prediction (solid line) of the hitting probability in Eq. (13) with $m = 1$ [more explicit form given in Eq. (56) in Ref. [78]], compared with the one evaluated numerically from the effective Langevin equation (2) (symbols) with $D = 1$ and $t_f = 1$. For a given m , it exhibits a unique maximum at $R = R^* \approx 1.671$ (red dot). Right panel: The theoretical prediction (solid line) of the rescaled expected maximum $\langle M(t_f) \rangle = \sqrt{\pi D t_f} q(R = rt_f)$ in Eq. (69) in Ref. [78] compared with the one evaluated numerically (symbols) with $D = 1$ and $t_f = 1$. The function $q(R)$ has a maximum at $R^* \approx 2.153$. In both panels, we sampled 10^6 trajectories.

paradigm of an optimal resetting rate $R^*(m)$ is also manifest in the behavior of the hitting probability. As a function of the scaled target location m , the optimal rate $R^*(m)$ is also interesting (see Ref. [78]). Another observable that also confirms this optimal paradigm is the expected maximum of the RBB as a function of the rescaled resetting rate R that we have computed exactly in Ref. [78] (as shown in the right panel in Fig. 3).

To conclude, the principal result of this Letter is the uncovering of an unexpected mechanism of enhanced fluctuations, caused by the combined effect of the bridge condition and a small resetting rate. This mechanism is very general and holds in arbitrary dimensions. This enhanced fluctuation mechanism also leads to the existence of a resetting rate r^* that optimises the search process. This optimal paradigm holds in all dimensions but the mechanism for it is different from that of a standard resetting Brownian motion. An additional bonus of this Letter is to derive an exact effective Langevin equation in arbitrary dimensions that provides a complete rejection-free algorithm to generate numerically the trajectories of resetting Brownian bridges.

The trajectories have been generated with a time step of $dt = 10^{-3}$ and our code is available as a Julia notebook in Ref. [109].

We thank H. Orland for useful discussions. This work was partially supported by the Luxembourg National Research Fund (FNR) (App. ID 14548297).

-
- [1] F. Bartumeus and J. Catalan, *J. Phys. A* **42**, 434002 (2009).
 [2] G. M. Viswanathan, M. G. E. da Luz, E. P. Raposo, and H. E. Stanley, *The Physics of Foraging: An Introduction to Random Searches and Biological Encounters* (Cambridge University Press, Cambridge, England, 2011).

- [3] O. G. Berg, R. B. Winter, and P. H. von Hippel, *Biochemistry* **20**, 6929 (1981).
 [4] M. Coppey, O. Bénichou, R. Voituriez, and M. Moreau, *Biophys. J.* **87**, 1640 (2004).
 [5] S. Ghosh, B. Mishra, A. B. Kolomeisky, and D. Chowdhury, *J. Stat. Mech.* (2018) 123209.
 [6] D. Chowdhury, *Biophys. J.* **116**, 2057 (2019).
 [7] G. Adam and M. Delbrück, Reduction of dimensionality in biological diffusion processes, in *Structural Chemistry and Molecular Biology* (W.H. Freeman and Company, London, 1968).
 [8] W. J. Bell, *Searching Behaviour: The Behavioural Ecology of Finding Resources* (Chapman and Hall, London, 1990).
 [9] J. M. Wolfe and T. S. Horowitz, *Nat. Rev. Neurosci.* **5**, 495 (2004).
 [10] A. Montanari and R. Zecchina, *Phys. Rev. Lett.* **88**, 178701 (2002).
 [11] G. Oshanin, H. S. Wio, K. Lindenberg, and S. F. Burlatsky, *J. Phys. Condens. Matter* **19**, 065142 (2007).
 [12] E. Gelenbe, *Phys. Rev. E* **82**, 061112 (2010).
 [13] J. Snider, *Phys. Rev. E* **83**, 011105 (2011).
 [14] O. H. Abdelrahman and E. Gelenbe, *Phys. Rev. E* **87**, 032125 (2013).
 [15] M. Chupeau, O. Bénichou, and S. Redner, *Phys. Rev. E* **95**, 012157 (2017).
 [16] M. A. Lomholt, T. Koren, R. Metzler, and J. Klafter, *Proc. Natl. Acad. Sci. U.S.A.* **105**, 11055 (2008).
 [17] O. Bénichou, C. Loverdo, M. Moreau, and R. Voituriez, *Rev. Mod. Phys.* **83**, 81 (2011).
 [18] M. R. Evans, S. N. Majumdar, and G. Schehr, *J. Phys. A* **53**, 193001 (2020).
 [19] M. Villén-Altramirano and J. Villén-Altramirano, RESTART: A method for accelerating rare event simulations, in *Queueing Performance and Control in ATM (Proceedings of the 13th International Telegraphic Congress)*, edited by J. W. Cohen and C. D. Pack (Elsevier Science, Amsterdam, North-Holland, 1991).
 [20] M. Luby, A. Sinclair, and D. Zuckerman, *Inf. Proc. Lett.* **47**, 173 (1993).
 [21] H. Tong, C. Faloutsos, and J.-Y. Pan, *Knowl. Inf. Syst.* **14**, 327 (2008).
 [22] K. Avrachenkov, A. Piunovskiy, and Y. Zhang, *J. Appl. Probab.* **50**, 960 (2013).
 [23] J. H. Lorenz, Runtime distributions and criteria for restarts, in *SOFSEM2018: Theory and Practice of Computer Science*, edited by A. Tjoa *et al.*, Lecture Notes in Computer Science Vol. 10706 (Edizioni della Normale, Cham, 2018), pp. 493–507.
 [24] S. Reuveni, M. Urbakh, and J. Klafter, *Proc. Natl. Acad. Sci. U.S.A.* **111**, 4391 (2014).
 [25] T. Rotbart, S. Reuveni, and M. Urbakh, *Phys. Rev. E* **92**, 060101(R) (2015).
 [26] D. Boyer and C. Solis-Salas, *Phys. Rev. Lett.* **112**, 240601 (2014).
 [27] S. N. Majumdar, S. Sabhapandit, and G. Schehr, *Phys. Rev. E* **92**, 052126 (2015).
 [28] G. Mercado-Vasquez and D. Boyer, *J. Phys. A* **51**, 405601 (2018).
 [29] A. Masó-Puigdellosas, D. Campos, and V. Méndez, *Front. Phys.* **7**, 112 (2019).

- [30] A. Pal, L. Kusmierz, and S. Reuveni, *Phys. Rev. Research* **2**, 043174 (2020).
- [31] B. Levikson, *J. Appl. Probab.* **14**, 492 (1977).
- [32] A. G. Pakes, *J. Appl. Probab.* **15**, 65 (1978).
- [33] P. J. Brockwell, J. Gani, and S. I. Resnick, *Adv. Appl. Probab.* **14**, 709 (1982).
- [34] P. J. Brockwell, *Adv. Appl. Probab.* **17**, 42 (1985).
- [35] E. G. Kyriakidis, *Stat. Probab. Lett.* **20**, 239 (1994).
- [36] A. G. Pakes, *Commun. Stat. Stoch. Model.* **13**, 255 (1997).
- [37] S. C. Manrubia and D. H. Zanette, *Phys. Rev. E* **59**, 4945 (1999).
- [38] A. Economou and D. Fakinou, *Eur. J. Oper. Res.* **149**, 625 (2003).
- [39] P. Visco, R. J. Allen, S. N. Majumdar, and M. R. Evans, *Biophys. J.* **98**, 1099 (2010).
- [40] S. Dharmaraja, A. Di Crescenzo, V. Giorno, and A. G. Nobile, *J. Stat. Phys.* **161**, 326 (2015).
- [41] M. R. Evans and S. N. Majumdar, *Phys. Rev. Lett.* **106**, 160601 (2011).
- [42] M. R. Evans and S. N. Majumdar, *J. Phys. A* **44**, 435001 (2011).
- [43] S. Redner, *A Guide to First-Passage Processes* (Cambridge University Press, New York, 2001).
- [44] A. J. Bray, S. N. Majumdar, and G. Schehr, *Adv. Phys.* **62**, 225 (2013).
- [45] M. R. Evans and S. N. Majumdar, *J. Phys. A* **47**, 285001 (2014).
- [46] L. Kuśmierz, S. N. Majumdar, S. Sabhapandit, and G. Schehr, *Phys. Rev. Lett.* **113**, 220602 (2014).
- [47] C. Christou and A. Schadschneider, *J. Phys. A* **48**, 285003 (2015).
- [48] D. Campos and V. Méndez, *Phys. Rev. E* **92**, 062115 (2015).
- [49] M. Montero and J. Villarroel, *Phys. Rev. E* **94**, 032132 (2016).
- [50] A. Nagar and S. Gupta, *Phys. Rev. E* **93**, 060102(R) (2016).
- [51] A. Pal, A. Kundu, and M. R. Evans, *J. Phys. A* **49**, 225001 (2016).
- [52] S. Eule and J. J. Metzger, *New J. Phys.* **18**, 033006 (2016).
- [53] S. Reuveni, *Phys. Rev. Lett.* **116**, 170601 (2016).
- [54] A. Pal and S. Reuveni, *Phys. Rev. Lett.* **118**, 030603 (2017).
- [55] A. Chechkin and I. M. Sokolov, *Phys. Rev. Lett.* **121**, 050601 (2018).
- [56] M. R. Evans and S. N. Majumdar, *J. Phys. A* **51**, 475003 (2018).
- [57] A. Pal and V. V. Prasad, *Phys. Rev. Research* **1**, 032001(R) (2019).
- [58] A. Pal and V. V. Prasad, *Phys. Rev. E* **99**, 032123 (2019).
- [59] P. C. Bressloff, *J. Phys. A* **53**, 425001 (2020).
- [60] P. C. Bressloff, *J. Phys. A* **53**, 275003 (2020).
- [61] B. De Bruyne, J. Randon-Furling, and S. Redner, *Phys. Rev. Lett.* **125**, 050602 (2020).
- [62] B. De Bruyne, J. Randon-Furling, and S. Redner, *J. Stat. Mech.* (2021) 013203.
- [63] B. De Bruyne and F. Mori, [arXiv:2112.11416](https://arxiv.org/abs/2112.11416).
- [64] O. Tal-Friedman, A. Pal, A. Sekhon, S. Reuveni, and Y. Roichman, *J. Phys. Chem. Lett.* **11**, 7350 (2020).
- [65] B. Besga, A. Bovon, A. Petrosyan, S. N. Majumdar, and S. Ciliberto, *Phys. Rev. Research* **2**, 032029(R) (2020).
- [66] F. Faisant, B. Besga, A. Petrosyan, S. Ciliberto, and S. N. Majumdar, *J. Stat. Mech.* (2021) 113203.
- [67] D. D. Murphy and B. R. Noon, *Ecol. Appl.* **2**, 3 (1992).
- [68] L. Giuggioli, G. Abramson, V. M. Kenkre, G. Suzán, E. Marcé, and T. L. Yates, *Bull. Math. Biol.* **67**, 1135 (2005).
- [69] M. F. Shlesinger, *Nature (London)* **443**, 281 (2006).
- [70] J. Randon-Furling, S. N. Majumdar, and A. Comtet, *Phys. Rev. Lett.* **103**, 140602 (2009).
- [71] S. A. Boyle, W. C. Lourenco, L. R. Da Silva, and A. T. Smith, *Folia Primatol.* **80**, 33 (2009).
- [72] S. N. Majumdar, A. Comtet, and J. Randon-Furling, *J. Stat. Phys.* **138**, 955 (2010).
- [73] M. Muller and R. Wehner, *Proc. Natl. Acad. Sci. U.S.A.* **85**, 5287 (1988).
- [74] J. S. Horne, E. O. Garton, S. M. Krone, and J. S. Lewis, *Ecology* **88**, 2354 (2007).
- [75] J. W. Fisher, W. D. Walter, and M. L. Avery, *Condor* **115**, 298 (2013).
- [76] W. J. Morokoff and R. E. Caflisch, *Monte Carlo and Quasi-Monte Carlo Methods* (Springer, New York, 1998), p. 340.
- [77] O. Thas, *Comparing Distributions* (Springer, New York, 2009).
- [78] See Supplemental Material at <http://link.aps.org/supplemental/10.1103/PhysRevLett.128.200603> for detailed computations which includes Refs. [79–81].
- [79] S. N. Majumdar, S. Sabhapandit, and G. Schehr, *Phys. Rev. E* **91**, 052131 (2015).
- [80] L. C. G. Rogers and D. Williams, *Diffusions, Markov Processes and Martingales* (Cambridge University Press, Cambridge, England, 2000).
- [81] P. Billingsley, *Convergence of Probability Measures* (Wiley, New York, 1968).
- [82] J. L. Doob, *Bull. Soc. Math. Fr.* **85**, 431 (1957).
- [83] P. Fitzsimmons, J. Pitman, and M. Yor, *Seminar on Stochastic Processes* (Springer, Berlin, 1993).
- [84] P. G. Bolhuis, D. Chandler, C. Dellago, and P. L. Geissler, *Annu. Rev. Phys. Chem.* **53**, 291 (2002).
- [85] C. Giardinà, J. Kurchan, and L. Peliti, *Phys. Rev. Lett.* **96**, 120603 (2006).
- [86] C. Giardinà, J. Kurchan, V. Lecomte, and J. Tailleur, *J. Stat. Phys.* **145**, 787 (2011).
- [87] H. Orland, *J. Chem. Phys.* **134**, 174114 (2011).
- [88] R. Chetrite and H. Touchette, *Ann. Henri Poincaré* **16**, 2005 (2015).
- [89] S. N. Majumdar and H. Orland, *J. Stat. Mech.* (2015) P06039.
- [90] A. Mazzolo, *J. Stat. Mech.* (2017) 023203.
- [91] A. Mazzolo, *J. Math. Phys. (N.Y.)* **58**, 093302 (2017).
- [92] K. Klymko, P. L. Geissler, J. P. Garrahan, and S. Whitelam, *Phys. Rev. E* **97**, 032123 (2018).
- [93] J. P. Garrahan, *Physica (Amsterdam)* **504A**, 130 (2018).
- [94] E. Brunet, A. D. Le, A. H. Mueller, and S. Munier, *Europhys. Lett.* **131**, 40002 (2020).
- [95] D. C. Rose, J. F. Mair, and J. P. Garrahan, *New J. Phys.* **23**, 013013 (2021).
- [96] A. Das, D. C. Rose, J. P. Garrahan, and D. T. Limmer, *J. Chem. Phys.* **155**, 134105 (2021).

- [97] A. Chabane, A. Lazarescu, and G. Verley, *J. Stat. Phys.* **187**, 6 (2022).
- [98] A. Baldassarri, *J. Stat. Mech.* (2021) 083211.
- [99] J. Grela, S. N. Majumdar, and G. Schehr, *J. Stat. Phys.* **183**, 49 (2021).
- [100] B. De Bruyne, S. N. Majumdar, H. Orland, and G. Schehr, *J. Stat. Mech.* (2021) 123204.
- [101] C. Monthus, *J. Stat. Mech.* (2022) 023207.
- [102] B. De Bruyne, S. N. Majumdar, and G. Schehr, *Phys. Rev. E* **104**, 024117 (2021).
- [103] B. De Bruyne, S. N. Majumdar, and G. Schehr, *J. Phys. A* **54**, 385004 (2021).
- [104] E. Roldan and S. Gupta, *Phys. Rev. E* **96**, 022130 (2017).
- [105] V. P. Shkilev, *Phys. Rev. E* **96**, 012126 (2017).
- [106] R. G. Pinsky, *Stoch. Proc. Appl.* **130**, 2954 (2020).
- [107] S. Ray, *J. Chem. Phys.* **153**, 234904 (2020).
- [108] A. S. Bodrova and I. M. Sokolov, *Phys. Rev. E* **102**, 032129 (2020).
- [109] B. De Bruyne, <https://github.com/Bbruyne/RBB>.